Electronic Supplementary Material (ESI) for Journal of Materials Chemistry A.

SUPPORTING INFORMATION

In-situ lithiated quinone cathode for ALD/MLD-fabricated high-power thin-film battery

Mikko Nisula and Maarit Karppinen*

Department of Chemistry and Materials Science, Aalto University, FI-00076, Finland

*Corresponding author: maarit.karppinen@aalto.fi

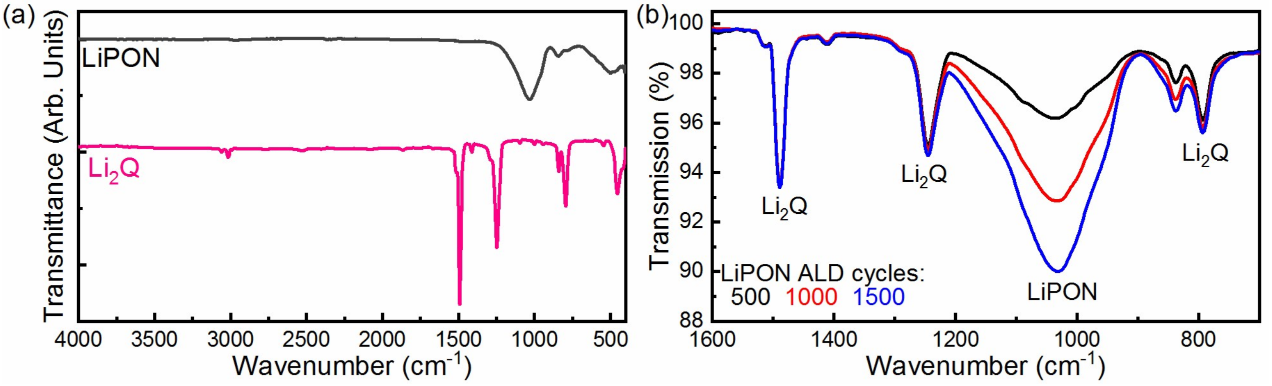

Figure S1. (a) Reference FTIR spectra of LiPON and Li_2Q. (b) FTIR spectra of the Li_2Q/LiPON stacks deposited on a silicon substrate, with the layer thicknesses being 100 ALD/MLD cycles for Li_2Q, and ranging from 500 to 1500 ALD cycles for LiPON.

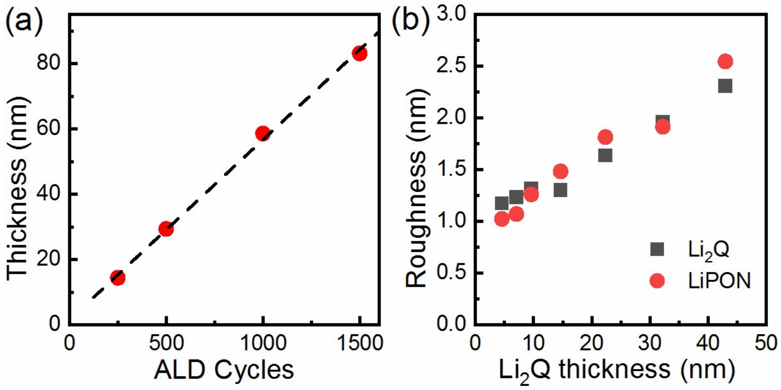

Figure S2. (a) The obtained layer thicknesses as a function of the number of ALD cycles LiPON (R^2 = 0.999) from the XRR data fitting. (b) The roughness values for Li2Q (grey squares) and LiPON (red circles) as a function of Li2Q layer thickness obtained from the XRR fit.

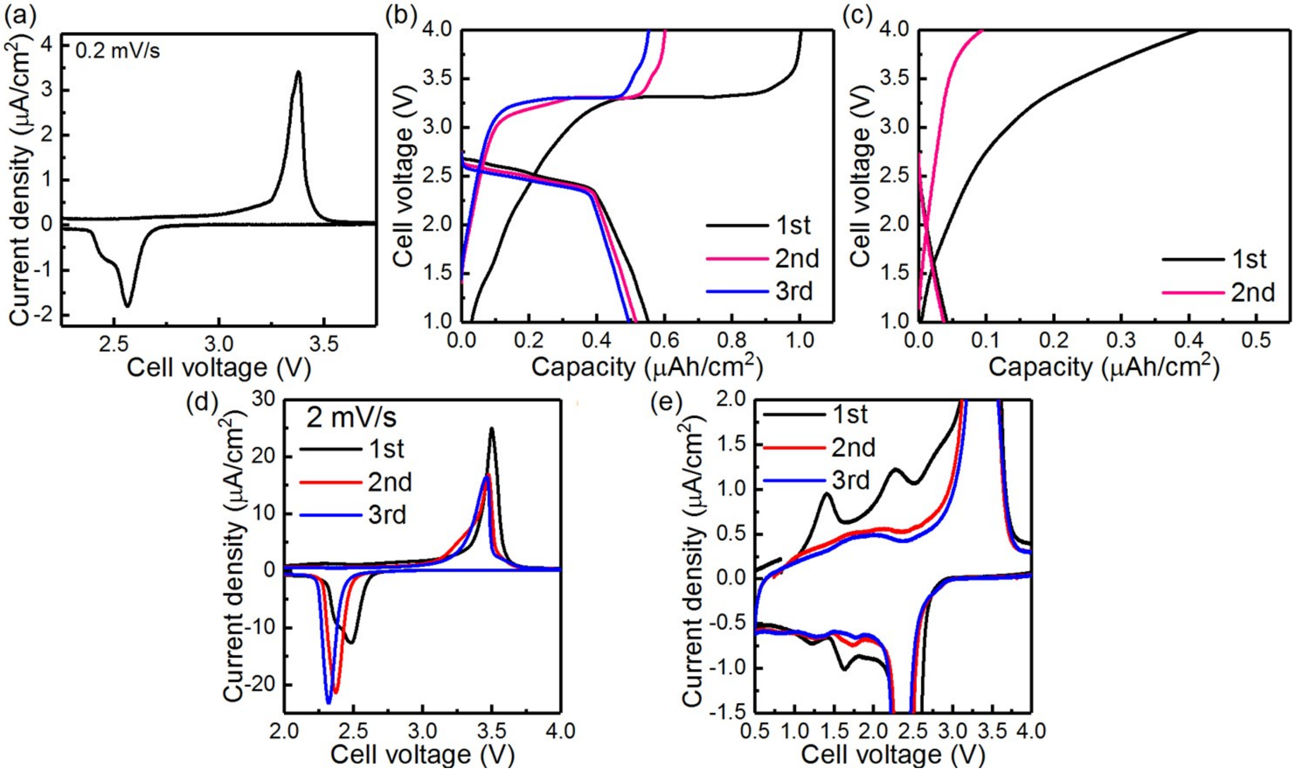

Figure S3. (a) Cyclic voltammogram of the solid-state cell at the scan rate of 0.2 mV/s. The sample thickness was 10 nm. (b) Chronopotentiometry plots of the first three charge-discharge cycles conducted at a current density of 2 μA/cm^2. The Li$_2$Q layer thickness was 10 nm. (c) The charge-discharge curves of a Pt/LiPON/Cu cells without the Li$_2$Q layer measured at current density of 2 μA/cm^2. (d) Cyclic voltammograms with three subsequent cycles at 2 mV/s (e) A close-up of the same graph.

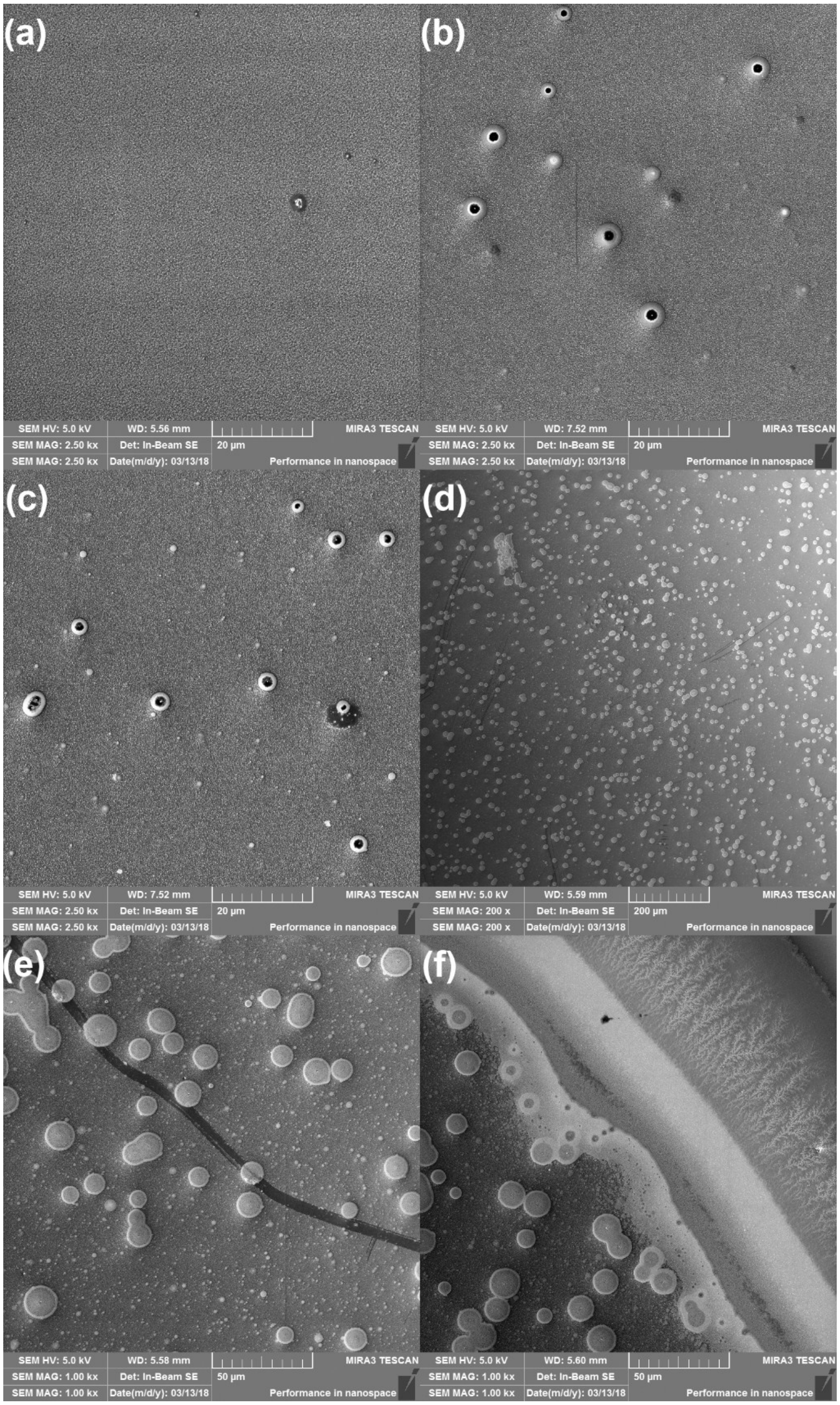

Figure S4. (a) Pristine cell, and a similar cell after (b) two charge/discharge cycles at 2 μA/cm^2, (c) one CV sweep at 0.2 mV/s (note the increased amount of deposits at the edges of the punctured current collector due to extended exposure time to trace O_2/H_2O in comparison to (b)), and (d) 20 cycles at 20 μA/cm^2. (e) Close-up showing the cracking of the current collector, and (f) degradation at the edge of the current collector with dendrite-like features extending from the current collector edge.

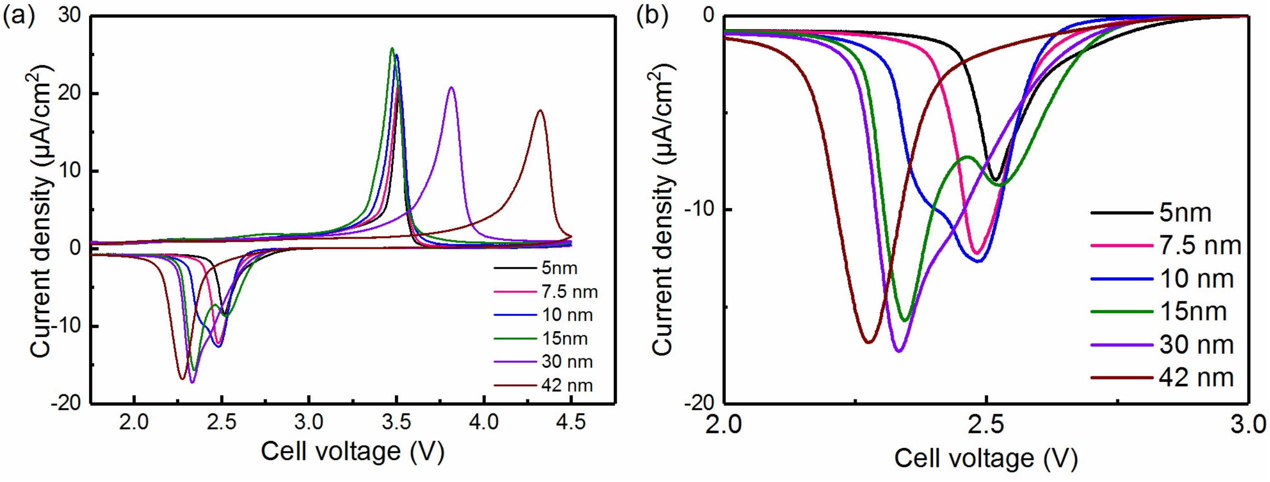

Figure S5. (a) Cyclic voltammograms of the solid-state cells with the Li_2Q layer thickness ranging from 5 to 42 nm. The scan rate was 2 mV/s. (b) Close-up of the reduction peaks showing minor (in comparison to the oxidation peak) but consistent shift to lower potentials.

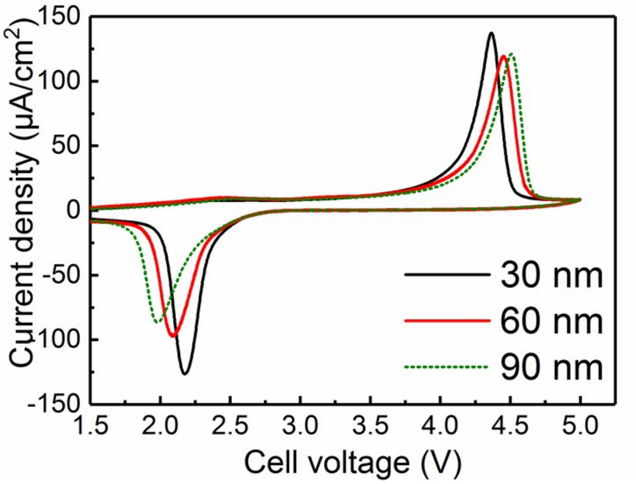

Figure S6. Cyclic voltammograms of the solid-state cells with the LiPON layer thickness ranging from 30 to 90 nm. The Li_2Q layer thickness was kept constant at 30 nm. The redox peak shift is symmetric and the integrated charge is uniform between the samples. The scan rate was 20 mV/s.

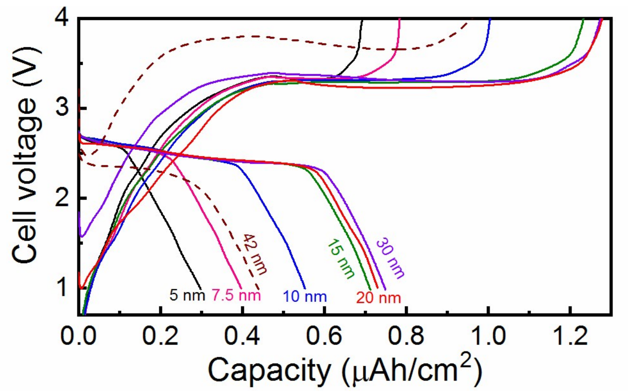

Figure S7. The effect of Li_2Q layer thickness on the charge-discharge voltage profiles conducted at a current density of 2 μA/cm^2. The capacity associated with the charge/discharge voltage plateaus are consistent with the redox peak areas of the corresponding cyclic voltammetry measurements shown in Figure S4.

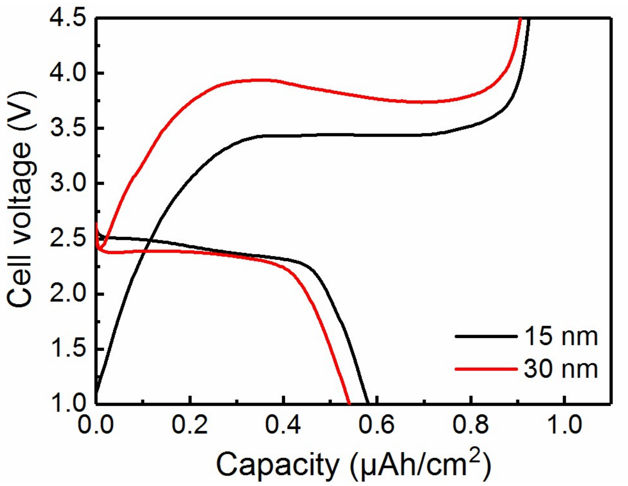

Figure S8. The effect of Li_2Q layer thickness on the charge-discharge voltage profiles conducted at a current density of 20 μA/cm^2.

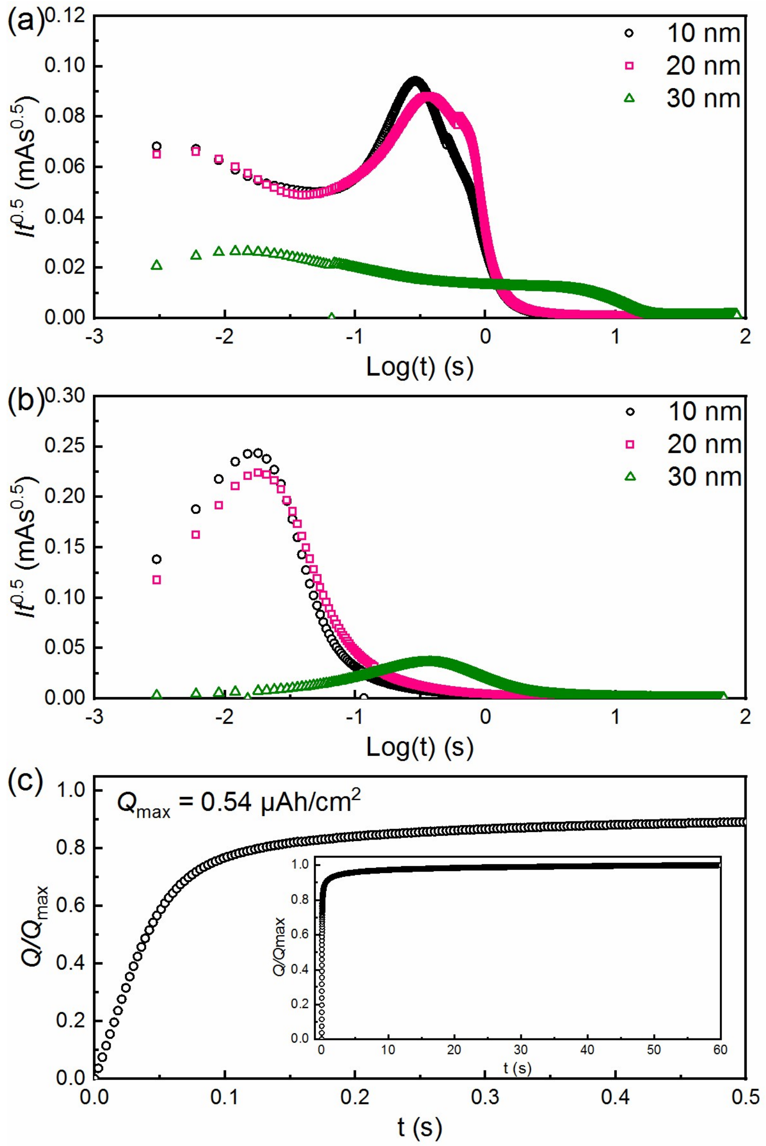

Figure S9. $It^{0.5}$ vs log *t* plots for (a) oxidation and (b) reduction of Li_2Q samples with thicknesses of 10 nm (black circles), 20 nm (red squares) and 30 nm (green triangles). For oxidation, the cell voltage was stepped from open circuit voltage to 4 V and held there for 60 s while measuring the current response. The reduction step to 1 V was then conducted after allowing the cells to relax for 5 min. (c) Integrated charge vs. t for the reduction of the 10 nm sample. The inset displays the full measurement time range.

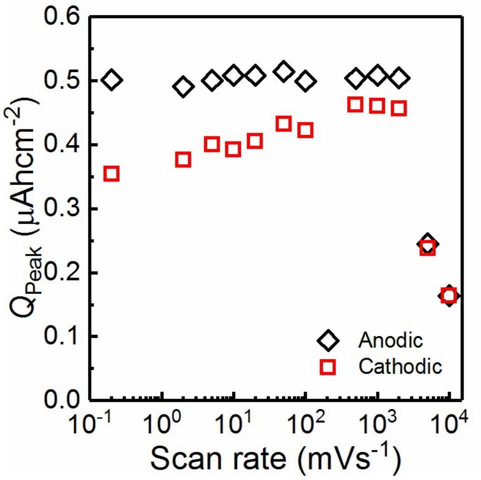

Figure S10. The integrated redox peak areas obtained from the first cycle (i.e. pristine cells) at each scan rate.

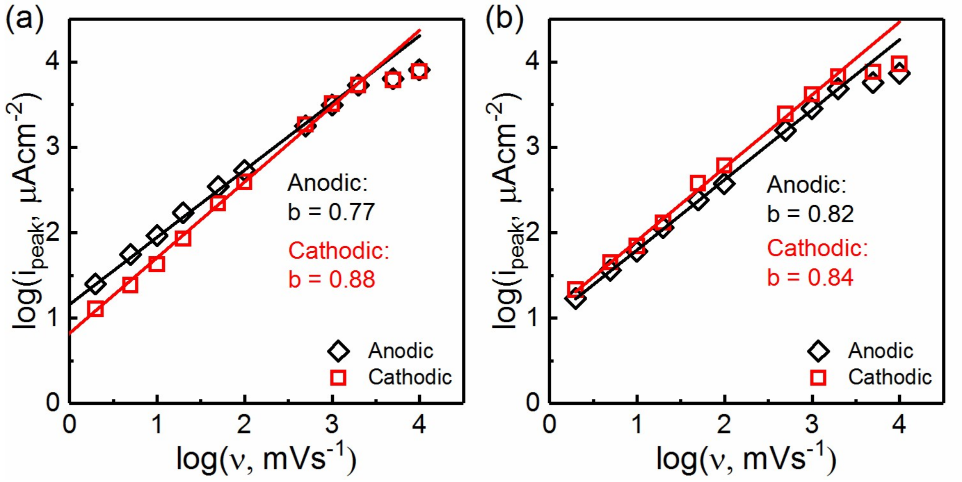

Figure S11. The log-log plots of the peak current dependency on the scan rate from (a) the first cycle (i.e. pristine cells), (b) the second cycle. The b-value signifies the slope of the plots.

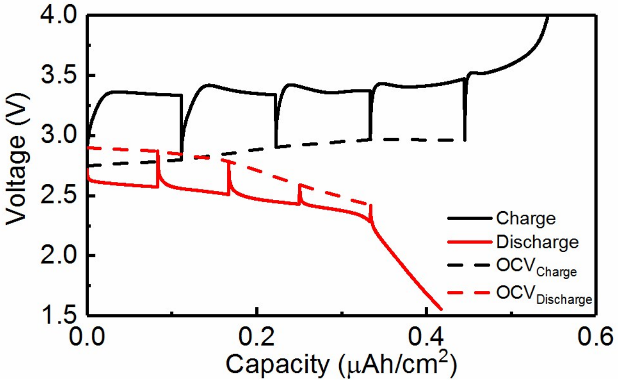

Figure S12. The galvanostatic intermittent titration technique (GITT) results with Li_2Q layer thickness of 10 nm. The solid lines represent the voltage response to 2μA/cm^2 current pulses applied for 200 s at a time (Black = charge, red = discharge). The dashed lines trace the open circuit voltage after 900 s of stabilization at the end of a current pulse. The measurement was limited to only 5 current pulses for both charge and discharge as the in-situ formed metallic lithium anode deteriorated upon extended exposure to the glove box atmosphere, here seen as partial loss of capacity upon discharge. The measurement was performed on a pristine cell, and the data shown here was preceded by constant current charge to 3 V to exclude the effect of the initial irreversible reaction associated with the solid electrolyte parasitic reaction.

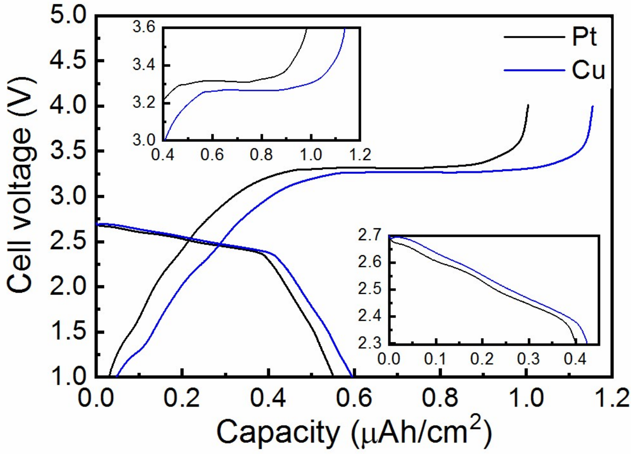

Figure S13. Effect of the positive electrode current collector on the charge/discharge voltages.

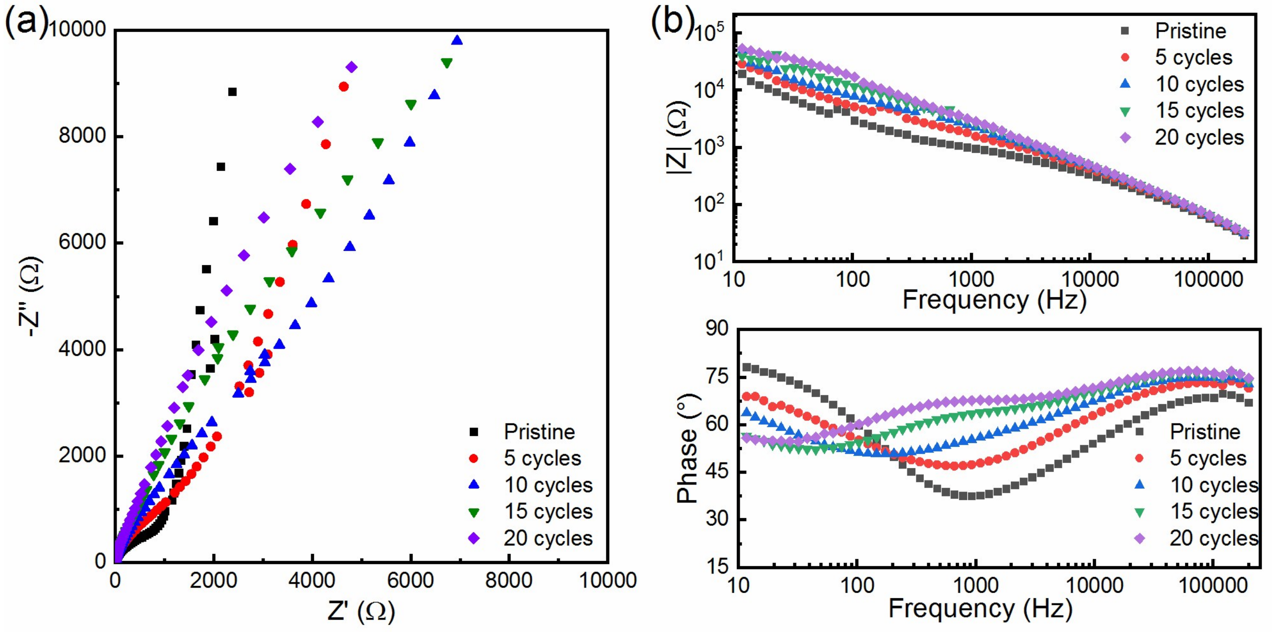

Figure S14. Electrochemical impedance spectroscopy (EIS) conducted at 5 charge/discharge cycle interval (a) Nyquist plot, (b) Bode plot of the same data. The measurements were conducted in the frequency range of 200 kHz - 10 Hz with an amplitude of 10 mV.